Revealing the neural networks that extract conceptual gestalts from continuously evolving or changing semantic contexts

Francesca M. BRANZI [1], Gina F. HUMPHREYS [1], Paul HOFFMAN [2], and Matthew A. LAMBON RALPH [1]

[1] MRC Cognition & Brain Sciences Unit, The University of Cambridge, 15 Chaucer Road, Cambridge CB2 7EF

[2] School of Philosophy, Psychology & Language Sciences, University of Edinburgh, Edinburgh, UK

Address for correspondence:
Francesca M. Branzi; Room 29, MRC Cognition & Brain Sciences Unit, The University of Cambridge
15 Chaucer Rd, Cambridge, CB2 7EF, E: Francesca.Branzi@mrc-cbu.cam.ac.uk

Or

Prof. Matthew A. Lambon Ralph; Room 25, MRC Cognition & Brain Sciences Unit,
The University of Cambridge, 15 Chaucer Rd, Cambridge, CB2 7EF, E: Matt.Lambon-Ralph@mrc-cbu.cam.ac.uk

Abstract

Reading the news, watching a movie or any other behaviour involving the processing of meaningful stimuli requires the semantic system to have two main features: being active during an extended period of time and flexibly adapting the internal representation according to the changing environment (e.g., change of semantic context). Despite being a key feature of many everyday tasks, formation and updating of the semantic "gestalt" are still poorly understood. In this fMRI study we used naturalistic stimuli and task manipulations to establish which brain areas reflect time-extended semantic combinatorial processes and distinguish them from those related to other cognitive processes (e.g., working memory and domain-general attention). Univariate and multivariate (ICA) techniques revealed various findings: firstly, time-extended formation and reset of the conceptual gestalt is reflected in the neurocomputations of the anterior temporal lobe. Secondly, semantic combinations are supported by a fronto-parietal network, possibly reflecting working memory for the integration of contextual information. Third, during the reset of the semantic gestalt, the ATL neurocomputations are accompanied by the recruitment of the multi-demand network, with a key role of brain structures in the right hemisphere, and other domain-general attentional neural systems. Finally, we show that rather than supporting semantic integration, the default mode network reflects down-regulation of brain regions that are irrelevant for the task. The implications of these findings for neurocognitive models of semantic cognition are discussed.

Keywords: semantic; context; narrative; fMRI; ICA.

SIGNIFICANCE STATEMENT: Real-life experiences consist of a continuous stream of perceptual meaningful stimuli. Hence, the semantic system is required over an extended-period of time to build a continuously evolving conceptual gestalt from the torrent of words and non-verbal stimuli. By using naturalistic stimuli with extended temporal structure, paired with a univariate and multivariate analyses, we identified the semantic neural network that extracts conceptual gestalts from continuously evolving and changing semantic contexts. Our findings highlight the important contribution of the right hemisphere to naturalistic semantic processing, contrast with accounts positing that DMN has crucial role in semantic integration, and reveal a network crucial for the integration of contextual information.

1. Introduction

Successful time-extended verbal and nonverbal semantic cognition (e.g., understanding the news reports on the radio or the sequential scenes in a silent movie) relies on the ability of the semantic system to integrate information over time to build meaningful representations of the evolving world around us. Although semantic integration is often error-free and apparently effortless, the cognitive challenges are non-trivial. Thus, the semantic system is required over an extended-period of time to build a continuously evolving conceptual gestalt from the torrent of words and non-verbal stimuli yet, when the context or situation changes (which is often not overtly signalled but has to be inferred), the semantic system has to reset and build a new conceptual gestalt afresh.

Despite being a core, everyday function of semantic cognition, the neural foundations of conceptual gestalt formation and resetting are still uncharacterised. In fact, a handful of studies have utilised word pairs to explore the formation of meaning at the noun-phrase level (e.g., 1,2) without addressing the time-extended demands posed by everyday semantic cognition. Other studies, instead, have measured multi-item semantic combinations without task manipulations that distinguish between brain structures involved in semantic integration from those involved in extra-semantic neurocomputations (e.g., working memory (WM), attentional control, etc.: e.g., 3,4,5,6).

Accordingly, in this functional magnetic resonance imaging (fMRI) study we established the brain networks that support time-extended semantic integration as well as those that are sensitive to changes in semantic context. These important research questions were addressed through a straightforward experimental design. First, we used combinations of short paragraphs to reflect the time-extended demands posed by everyday semantic cognition and the challenges posed by the formation of larger conceptual gestalts. Second, we adopted a key manipulation to determine the neural networks involved in the formation of the conceptual gestalt and to differentiate them from brain structures supporting extra-semantic control mechanisms. Thus, participants were asked to read short narratives composed of two phases (context and target). For each narrative, the same second paragraph (target) was preceded by different types of context: (i) a highly congruent context (HC) which maximised the information contained in a single coherent gestalt; (ii) a low-congruent (LC) paragraph with a divergent meaning, thus testing the semantic system's ability to reformulate/reset the context (see Table S1); and (iii) a no context control (NC) in which the same target was preceded by a number reading task (thus requiring a more substantial shift from a non-semantic to semantic task). The resultant fMRI data were analysed only for the identical target paragraph thus ensuring that any observed differences must reflect the influence of the preceding contexts (the periods covering these

contexts were not included in the fMRI analyses). To establish the key brain areas and networks, we used both univariate and multivariate (independent component analysis; ICA) analyses.

We expected to observe brain areas already implicated in semantic cognition as well as additional networks that might reflect the demands posed by computing and resetting conceptual contexts. A large body of cognitive and clinical neuroscience research, based primarily on the processing and representation of single concepts, has identified two interactive neural networks (7). The first builds coherent, generalizable, multimodal conceptual representations through the interaction of an anterior temporal lobe (ATL) hub with a distributed set of secondary association cortices (8,9). The computational models of this network (9,10,11) have always emphasised that the ATL hub allows information to be combined into coherent concepts from across verbal and nonverbal sources (words, sounds, vision, etc.) and also over time. Accordingly, it seems entirely possible that this network would be important for the formation of the conceptual gestalts conveyed in the narratives. Indeed, a handful of previous studies have found evidence for a combinatorial semantic process in the superior ATL (e.g., 12,13,14,15,16).

The second established semantic network reflects the need to shape and mould semantic information to align with changing tasks demands (e.g., 17). This executive semantic network is comprised of prefrontal, posterior middle temporal and intraparietal sulcus areas (18,19). It seems likely that this second network will be important in processing the meaning of the narratives, especially when there is a shift in the context.

Given the cognitive requirements posed by the formation of meaning across a complete narrative, additional networks are likely to be engaged. Consistent with previous findings (3,4,6, 20,21,22,23), a network comprising midline brain regions and the angular gyrus (AG) may be sensitive to semantic integration and, possibly, to changes of semantic context (24,25).

ICA provides a data-driven approach for identifying independent spatiotemporal networks, which can then be tested for their sensitivity to the experimental conditions included in the fMRI task. Thus, ICA is particularly useful for revealing which brain structures are recruited simultaneously for semantic integration. Task-active and resting-state fMRI reveal multiple spatiotemporal networks including a semantic-language network (SLN), an executive control network (ECN), a default-mode network (DMN), etc. (e.g., 26,27,28,29). Some of these networks overlap with the hypothesised neural networks for semantic representation and control (see above). Accordingly, we expected these to be engaged by the task and to be sensitive to the context congruency. The networks associated with dorsal executive and semantic control should be critically important for resetting the semantic context, as they have been shown to engage whenever semantic processing is demanding (5,18,30) or after changes of non-semantic rules (31). Furthermore, the DMN – which is often anticorrelated with the

dorsal executive network (32,33,34,35, but see 36) – might also be a crucial network for the formation of conceptual gestalts. Its exact role, though, is hard to predict from the current literature on the DMN. Some researchers have suggested that the DMN may support processes for semantic integration (3,4,5,6,27), which would align with the seminal work of Binder that 'rest' involves considerable spontaneous semantic-language activities (37). More recent evidence indicates that this hypothesis holds for nodes within the semantic network, such as the ATL, but the AG and other aspects of the DMN are deactivated by semantic and non-semantic tasks alike (19,32). According to the proposal that DMN is actively involved in the formation of semantic gestalt, it should be positively engaged during semantic processing, in a way proportional to the amount (HC&LC>NC) and congruency (HC>LC) of the semantic information to be integrated.

In contrast, explorations of episodic memory have implicated the AG and DMN in vivid episodic retrieval and buffering (38,39,40,41). Accordingly, it is possible that this buffering mechanism might be engaged by the time-extended narratives whilst participants build up a mental model for the story based on the pre-existing context/schema (i.e., during HC and LC conditions only), predicting greatest activation for the consistent context condition (31,40). Also this hypothesis is in accord with evidence showing that the DMN is modulated by time-extended semantic integration (3,6). Finally, an alternative hypothesis with an opposing prediction arises from recent studies that suggest that the DMN is engaged when switching between activities (24,25). If correct, then the DMN should be most engaged by the NC condition where participants switch from a number to language activity.

2. Results

2.1. Behavioural results

The reading times (RTs) showed the expected behavioural effect of semantic coherence. Thus performance differed across experimental conditions [$F(2,46)=7.109$, $p=0.002$, $\eta p^2=0.236$], with reading speed in the NC and LC conditions being slower than in the HC condition ($p=0.008$ and $p=0.019$, respectively). There was no significant difference for reading the target sentence after the NC or LC contexts ($p>0.999$).

The percentage of given responses was very high and similar across all experimental conditions [$F(2,46)=2.521$, $p=0.091$, $\eta p^2=0.099$], with a trend towards significance for percentage of given responses in the HC condition being higher than in the NC condition ($p=0.098$) (Figure 1).

As mentioned in the Materials and Methods section, two participants were excluded from the fMRI analyses. Hence, we also ran behavioural analyses for these 22 participants. The results remained unchanged from those reported above for both RTs [$F(2,42)=5.491$, $p=0.008$, $\eta p^2=0.207$; NC>HC ($p=0.02$); LC>HC ($p=0.05$); NC=LC ($p>0.999$)] and percentage of given responses [$F(2,42)=2.841$, $p=0.07$, $\eta p^2=0.119$; NC<HC ($p=0.077$); LC=HC ($p>0.999$); NC=LC ($p=0.524$)].

2.2. fMRI results

2.2.1. *General Linear Modelling (GLM) results*

The Semantic Network

Whole-brain univariate analysis revealed that semantic reading tasks (target conditions) against rest or non-semantic reading tasks (number reading context) recruit a similar network of brain areas (Figure 2 and Table S2). This network includes frontal, temporal, and parietal brain areas, previously identified as key regions supporting semantic cognition (7). Furthermore, time-extended reading tasks recruit extensively also the right hemisphere and other areas, normally deactivated during semantic tasks (e.g., hippocampus, precuneus, and the mid-PGp subportion of the left AG) (19,32,42).

To determine which parts of the semantic network were sensitive to task manipulations, a set of independently-derived regions of interest (ROIs) (Table S3) were employed. These ROIs included ventral and dorsal portions of the ATL, left AG, posterior middle temporal gyrus (pMTG), inferior frontal gyrus (IFG), and anterior cingulate cortex/pre-supplementary motor area (ACC/pre-SMA) (Figure 2).

Temporal lobe ROIs. The anterior middle temporal gyrus (MTG~BA21) showed significantly increased responses for conditions with integration (HC and LC conditions) and particularly for coherent semantic endings (HC condition) [Left MTG: $F(2,42)=19.697$, $p<0.001$, $\eta p^2=0.484$; LC>NC ($p=0.003$), HC>NC ($p<0.001$), and LC<HC ($p=0.053$); Right MTG: $F(2,42)=19.536$, $p<0.001$, $\eta p^2=0.482$; LC>NC ($p=0.02$), HC>NC ($p<0.001$), and LC<HC ($p=0.028$)]. The anterior superior temporal gyrus (aSTG~BA38) showed increased neural responses for paragraphs preceded by a contextual support as compared with paragraphs without contextual integration (NC condition) [Left aSTG: $F(2,42)=18.449$, $p<0.001$, $\eta p^2=0.468$; LC>NC ($p=0.002$), HC>NC ($p<0.001$) and LC=HC ($p=0.162$); Right aSTG: $F(2,42)=24.682$, $p<0.001$, $\eta p^2=0.54$; LC>NC ($p=0.001$), HC>NC ($p<0.001$) and LC=HC ($p=0.108$)]. Finally, the inferior temporal gyrus (ITG~BA20) showed also sensitivity to integration of the contextual support [Left ITG: $F(2,42)=9.536$, $p<0.001$, $\eta p^2=0.312$; LC>NC ($p=0.049$), HC>NC ($p=0.002$), and LC=HC ($p=0.325$); Right ITG: $F(2,42)=9.172$, $p<0.001$, $\eta p^2=0.304$; LC>NC ($p=0.076$), HC>NC ($p=0.002$), and LC=HC ($p=0.178$)]. However, this ventral and medial portion of the ATL was not similarly engaged across all experimental conditions. Precisely, negligible responses were observed for NC condition [left ITG: $t(21)=1.36$, $p=0.188$; Right ITG: $t(21)=-0.605$, $p=0.552$] and for LC condition in the right hemisphere [$t(21)=1.537$, $p=0.139$], suggesting that this area is mostly engaged during integration of coherent semantic information (HC condition).

Left AG ROIs. The three different left AG spheres revealed the same type of semantic integration pattern, in that they were most active for the HC condition and least for the NC condition [mid-PGp: $F(2,42)=17.575$, $p<0.001$, $\eta p^2=0.456$; LC>NC ($p=0.009$), HC>NC ($p<0.001$), and LC=HC ($p=0.16$); ventral PGa: $F(2,42)=21.759$, $p<0.001$, $\eta p^2=0.509$; LC>NC ($p=0.006$), HC>NC ($p<0.001$), and HC>LC ($p=0.015$); dorsal PGa: $F(2,42)=13.126$, $p<0.001$, $\eta p^2=0.385$; LC>NC ($p=0.002$), HC>NC ($p=0.001$) and LC=HC ($p>0.999$)]. However, whilst the ventral PGa region was positively activated for NC conditions, the mid-PGp and dorsal PGa exhibited negligible activation for the NC conditions (one sample t-tests revealed ps>0.05 for NC conditions).

Semantic control network ROIs. The effect of shift of semantic context was predominantly observed in the right hemisphere. The right IFG (~BA47) [$F(2,40$[1]$)=8.039$, $p=0.001$, $\eta p^2=0.287$; LC>NC ($p=0.004$), HC=NC ($p>0.999$), and LC>HC ($p=0.017$)] and the right dAG [$F(2,42)=9.372$, $p<0.001$, $\eta p^2=0.309$; LC>NC ($p=0.004$), HC=NC ($p>0.999$), and LC>HC ($p=0.007$)] showed increased responses for LC>HC conditions.

[1] Data from one participant were excluded from the statistical analysis in right IFG (~BA47) and left ACC/pre−SMA as they were identified as outliers (Tukey's outlier detection rule).

With the exception of the left ACC/pre-SMA (~BA32/8/6) [F(2,40)=6.822, p=0.003, ηp^2=0.254; LC>NC (p=0.017), HC=NC (p>0.999), and LC>HC (p=0.015)], the LC>HC difference was not observed in the left hemisphere [left IFG (~BA45/44): F(2,42)=5.326, p=0.009, ηp^2=0.202; LC>NC (p=0.047), HC=NC (p=0.145), LC=HC (p=0.324); left pMTG (~BA21/37/20): F(2,42)=1.963, p=0.153, ηp^2=0.086; left IFG (~BA47): F(2,42)=4.269, p=0.021, ηp^2=0.169; LC>NC (p=0.043), HC=NC (p=0.289), and LC=HC (p=0.537)]. Finally, the right IFG (~BA44/45) showed a context integration effect [F(2,42)=8.098, p=0.001, ηp^2=0.278; LC>NC (p=0.01), and HC>NC (p=0.088), and LC=HC (p=0.102)].

The independent ROI analyses revealed three key findings: first, the gyral distribution of semantic task activation in the temporal lobe supported previous research and revealed novel insights on the functional specialisation of the ATL for time-extended combinatorial processes. As expected, we observed a bilateral involvement of the ATL in semantic processing (19,30,43,44). Interestingly, the effect of semantic coherence (HC>LC) was observed in the MTG. The aSTG and ITG showed a general effect of semantic integration (HC&LC>NC), as they were engaged more strongly – or uniquely in the case of ITG – for those condition preceded by a context paragraph (i.e., LC and HC conditions). Secondly, the re-setting of the semantic system (LC>HC) engages brain structures generally recruited when semantic processing requires increased executive control demands (18). However, differently from previous studies, these effects are mainly observed in the right hemisphere. Finally, as found in many previous studies (32,42,45,46), the response profile in AG was found to shift rapidly and quickly across the AG region. The anterior ventral portion (vPGa) was sensitive to the semantic coherence of the information to be integrated, whereas instead dPGa and mid-PGp were not. Instead, these two AG sub-regions showed a semantic integration effect as they were engaged only for those condition preceded by a semantic contextual support (i.e., LC and HC conditions).

Whole-brain univariate analyses of the differences between experimental conditions

Semantic Integration effect. Both high and low congruity conditions generated very similar, overlapping neural semantic networks including different portions of the dorsal ATL, extending to posterior portions of the superior temporal sulcus (pSTS), ventral portions of the AG (vPGa) and bilateral IFG (Figure 3, and Table S2). Furthermore, the overlap was also observed in correspondence of "extra-semantic" areas, i.e., areas that are not referred in the literature to semantic cognition in particular, such as the hippocampus, the right AG, medial superior frontal gyrus (mSFG) and the precuneus/posterior cingulate cortex (PCC).

Given neural responses within the semantic network were extensively investigated (see Figure

2), the following ROI analysis focussed on overlapping extra-semantic regions in order to reveal their role in semantic integration. Similar to portions of the AG (Figure 2B), the semantic integration effect in these areas was driven by qualitative rather than quantitative differences between conditions. In fact, the precuneus/PCC (x=±9, y=-54, z=36) [Left:$F(2,42)=17.632$, $p<0.001$, $\eta p^2=0.456$; LC>NC ($p=0.005$), HC>NC ($p<0.001$), and LC=HC ($p=0.391$); Right: $F(2,42)=14.644$, $p<0.001$, $\eta p^2=0.411$; LC>NC ($p=0.002$), HC>NC ($p<0.001$), and LC=HC ($p>0.999$)], the left hippocampus (x=-24, y=-9, z=-24) [$F(2,42)=9.246$, $p<0.001$, $\eta p^2=0.306$; LC>NC ($p=0.024$), HC>NC ($p<0.001$), and LC=HC ($p>0.999$)], the right AG (vPGa/mid-PGp; x=54, y=-60, z=27) [$F(2,42)=15.420$, $p<0.001$, $\eta p^2=0.423$; LC>NC ($p<0.001$), HC>NC ($p=0.001$), and LC=HC ($p>0.999$)] and the right mSFG (~BA9/32; x=6, y=48, z=39) [$F(2,42)=9.538$, $p<0.001$, $\eta p^2=0.312$; LC>NC ($p=0.014$), HC>NC ($p=0.002$), and LC=HC ($p>0.999$)] were all positively engaged for LC and HC conditions (see Figure 3A), but not for NC condition (one sample t-tests revealed all ps>0.05 for NC condition).

To summarise these results, integration of meaning across a narrative engages areas of the semantic network (see 7) as well as other brain regions. Unlike the semantic network regions, these extra-semantic areas are recruited only when contextual information can be integrated.

Shift of semantic and task contexts. The ACC/pre-SMA and the precuneus were activated more for the LC than HC condition. These regions were joined by other frontoparietal MD regions (47) (e.g., lateral IFG and superior parietal areas) and the right pMTG (Figure 3B and Table S2). ROI analysis established that LC>HC differential activation measured in a dorsal portion of the right precuneus (~BA7; x=12, y=-72, z=42) [$F(2,42)=11.472$, $p<0.001$, $\eta p^2=0.353$; LC=NC ($p>0.999$), HC<NC ($p=0.002$), and HC<LC ($p<0.001$)], in the right dAG (~BA40/39; x=42, y=-51, z=45) [$F(2,42)=8.862$, $p=0.001$, $\eta p^2=0.297$; LC>NC ($p=0.011$), HC=NC ($p=0.652$), and LC>HC ($p=0.006$)] and in the right ACC/pre-SMA (~BA32/8; x=3, y=30, z=42) [$F(2,42)=7.938$, $p=0.001$, $\eta p^2=0.274$; LC>NC ($p=0.016$), HC=NC ($p>0.999$), and LC>HC ($p=0.007$)] were all due to differential negligible or task-negative activation patterns.

Instead, other areas such as the left IFG (~BA44; x=-45, y=12, z=33) [$F(2,42)=9.781$, $p<0.001$, $\eta p^2=0.318$; LC>NC ($p=0.003$), HC=NC ($p=0.164$), and LC>HC ($p=0.036$)], the right insula (~BA47; x=30, y=24, z=6) [$F(2,42)=4.826$, $p=0.013$, $\eta p^2=0.187$; LC=NC ($p=0.243$), HC=NC ($p=0.366$), and LC>HC ($p=0.049$)] and the right pMTG (~BA21/20; x=60, y=-42, z=-6) [$F(2,40)=14.066$, $p<0.001$, $\eta p^2=0.413$; LC>NC ($p<0.001$), HC=NC ($p=0.125$), and LC>HC ($p=0.003$)], showed that the LC>HC effect reflected differences in positive activation levels. The HC>LC contrast did not reveal significant results.

Finally, we directly compared the NC>HC condition to establish which brain regions are

important for task switches into language from a non-language task (number reading) and therefore to identify possible similarities between neuro-computations supporting shifts of semantic and task contexts. This contrast activated a right lateralised set of higher-order visual regions, including also a portion of the right precuneus (see Figure 3B and Table S2) activated by the LC>HC contrast.

To summarise, resetting the conceptual gestalt elicits a robust activation of a bilateral set of frontal regions and the right pMTG. The right precuneus was less deactivated for LC and NC conditions as compared with HC condition, a pattern that mirrored that of RTs (see Figure 1).

2.2.2. Task group spatial ICA results

Task-related Functional Networks (FNs). ICA was used to explore which semantic and extra-semantic areas, revealed by univariate analyses, exhibited yoked activations – i.e., constituted functional networks rather than independent areas. ICA identified 22 independent components (IC), of which 5 exhibited significant sensitivity to our task conditions: These were a semantic/language network (SLN), an executive control network (ECN) including fronto-parietal regions, a higher visual network (HVN), a primary visual network (PVN), and a DMN (Figure 4 and Table S4).

As well as a bilateral set of semantic brain areas, the SLN included extra-semantic regions, suggesting that these regions are recruited together with semantic areas to support time-extended semantic cognition. Statistical analyses on the beta-weights revealed that the SLN was positively engaged by all three conditions (in comparison to rest), but that it was most active when the semantic context shifted (i.e., LC condition) [$F(2,42)=7.559$, $p=0.002$, $\eta p^2=0.265$; LC>NC ($p=0.007$), LC>HC ($p=0.032$)]. A related pattern was observed in the ECN which was positively engaged by both the HC and LC conditions, i.e., when a previous semantic context was available for integration [$F(2,42)=21.543$, $p<0.001$, $\eta p^2=0.506$; LC>NC ($p<0.001$), HC>NC ($p<0.001$)], though this was independent of whether the context was semantically congruent with the target or not [HC=LC ($p=0.774$)]. The two visual networks (HVN and PVN), containing occipital but also attentional control regions, were recruited most heavily for the NC condition, in which there was a change in the cognitive task [HVN: $F(2,42)=92.404$, $p<0.001$, $\eta p^2=0.815$; LC>NC ($p<0.001$), HC>NC ($p<0.001$) and LC>HC ($p<0.001$); PVN: $F(2,42)=59.467$, $p<0.001$, $\eta p^2=0.739$; LC>NC ($p<0.001$), HC>NC ($p<0.001$) and LC>HC ($p=0.001$)].

Finally, unlike the four other components, the DMN was deactivated with respect to rest. It exhibited sensitivity to the task conditions, in that it was least deactivated in the HC condition [$F(2, 42)=5.513$, $p=0.007$, $\eta p^2=0.208$; HC>NC ($p=0.025$), HC>LC ($p=0.063$); NC=LC ($p=0.88$)]. This pattern of deactivation mirrors the task performance (see Figure 1), in which RTs for the target

narrative were slowest for the LC and NC condition, and might reflect the common pattern that the degree of deactivation in the DMN is often correlated with task/item difficulty and other measures of behavioural stability (19,31,48,49). A negative correlation between averaged DMN time-courses (TCs) (averaged across runs and time-courses) and averaged RTs was observed in our study, without however reaching statistical significance (r=-0.099, p=0.662).

Functional network connectivity (FNC) analysis. Given our interest in studying the interaction between the SLN and other networks involved in time-extended semantic cognition, we computed a FNC analysis (see Figure S1). Significant positive correlations were observed between the TCs of DMN and SLN (r=0.13) and between DMN and ECN (r=0.23). Instead, the DMN was negatively correlated with HVN (r=-0.22). The ECN, the network not engaged during changes of task context, but only during semantic integration, showed a significant negative correlation with both HVN and PVN (r=-0.17 and r=-0.18, respectively), i.e., the networks maximally engaged during changes of task context (NC condition). In contrast with ECN, the SLN was positively correlated with both the HVN and PVN (r=0.28 and r=0.21, respectively). Finally, the TCs of the two visual networks were positively correlated (r=0.41).

These results may suggest that time-extended semantic integration is supported by both the SLN and ECN, interacting with the visual networks in different ways. Unlike the SLN, ECN recruitment is anticorrelated with the visual FNs, being strongly recruited when switching from number to text reading (NC conditions, i.e., shift of task context). Thus, it might be that switching efficiently from a non-semantic to a semantic task requires the activation of semantic and language areas (SLN) and, at the same time, the disengagement of brain regions involved in integration of contextual information (ECN). To test this hypothesis, we assessed whether the HVN-SLN positive coupling and the HVN-ECN negative coupling were negatively correlated with the behavioral cost of changing task context (operationalized as the difference between NC and HC conditions calculated for both % of missing rates and RTs). Given recent findings (24,25), we also tested whether this correlation could be observed with the HVN-DMN coupling.

Results revealed that the stronger the positive coupling between HVN and SLN, the smaller the behavioural cost associated with changes of task context (NC>HC % of missing rates) (r=-0.389, p=0.07) (Figure S1 B). Despite the correlation between the HVN-ECN coupling and the same behavioural cost was not significant (r=-0.121, p=0.59), we found that the HVN-DMN negative coupling was negatively correlated with the behavioural cost associated with changes of task context (NC>HC % of missing rates) (r=-0.373, p=0.08). The same correlation analyses were conducted with behavioural costs measured as RTs. However, these analyses did not reveal significant results or trends toward significance.

3. Discussion

Using both univariate and multivariate data-driven (ICA) approaches we revealed the brain regions and the networks supporting time-extended formation and resetting of conceptual representations. Unlike prior investigations (3,4,5,6), in this fMRI study we established which neural networks are primarily evoked by the formation and updating of semantic representations, and we distinguished them from those that support a semantic combinatorial neurocomputation. The main findings on the functional specialisation of brain areas within and outside the classical semantic network are discussed below, followed by discussion on the FNs, i.e., how semantic and extra-semantic regions are recruited together during meaning formation and update.

The Semantic Network

We hypothesised that the building of the conceptual gestalt would be supported by two interactive neural systems, reflecting representational and control aspects of semantic cognition, respectively. In accord with our hypothesis and previous findings (3,4,20), our results revealed that integrating semantic information during narrative processing engages a bilateral set of frontal, parietal and temporal brain structures, known as the "semantic network" (7). Within this network we identified hubs for formation of coherent concepts and control regions for context-sensitive regulation of semantic information.

Hubs for the formation of time-extended conceptual gestalt: the role of ATL

A first important result obtained from the univariate analysis is that the ATL supports neurocomputations for time-extended combinatorial semantics in addition to basic semantic combinations shown in previous studies (12,44), corroborating the hypothesis that this region is a key hub for the formation of conceptual representations (7,15,16,50). In particular, the effect of semantic coherence (HC>LC) was observed in the MTG, suggesting that this subregion of the ATL may have a crucial role in the formation of time-extended conceptual gestalt. Future studies will have to assess whether this effect is observed in other ATL areas when stimuli are presented in non-verbal modalities. In contrast, the aSTG and the ITG showed a general effect of semantic integration (HC&LC>NC) as they were engaged more strongly – or uniquely in the case of ITG – for those condition preceded by a context paragraph (i.e., LC and HC conditions).

The graded differential distribution of activation patterns observed within the ATL may reflect differences of structural connectivity between ATL subregions and primary input/output areas (51).

The lack of sensitivity for NC conditions in the ITG indicates that neural activity in this ATL subregion is modulated by the presence of contextual information. This effect may be determined because of direct connections (via entorhinal cortex) with regions supporting the formation of contextual memories, such as in the parahippocampal gyrus and the hippocampus (52,53,54). A recent study has demonstrated the interplay between semantic processing in ATL and information encoding/retrieval in the hippocampus during the formation/retrieval of contextual memories (55). Accordingly, it is possible that these anatomical connections allow these regions to cooperate for the formation and retrieval of semantic and contextual information conveyed in the narrative (e.g., episodic details), facilitating the flow of neocortical information into the hippocampus during encoding and the propagation of hippocampal retrieval signals into the ATL during retrieval. Future experimental studies combining high-temporal and high-spatial resolution techniques will be needed to test this possibility.

Brain regions for controlled integration of time-extended conceptual information: the contribution of the right hemisphere

A second important result is that increased semantic integration demands elicit bilateral activation of ventral and dorsal portions of the frontal lobe (Figure 3B). This result is in accord with previous studies that have employed tasks requiring multi-item combinations (5,20). Conversely, it differs from others that have utilised semantic association tasks, where the involvement of the IFG was mostly left lateralised (18,19).

The involvement of the right hemisphere during natural-like language processing has been attributed to the complexity of the input. In other words, as language input gets increasingly complex, there is increasing involvement of right hemisphere homologues to classic left hemisphere language areas (56). Particularly, the right hemisphere activation may become prominent and sustained when words and sentences are presented in a narrative context, and may here reflect coherence and inference at the propositional level and beyond, when readers make connections between sentences and paragraphs to form a coherent conceptual gestalt. This interpretation is in accord with the view that the right hemisphere, as compared to the left, would be involved in processing global aspects of linguistic contents, integrated over longer periods of time (57,58,59).

Nevertheless, this proposal does not entirely fit with our results since some key nodes within the semantic control network (i.e., dAG, pMTG and ventral IFG) show enhanced responses in the right, but not in the left hemisphere when integration requires major revision of the semantic context (LC>HC condition). Hence, despite the modulation of control regions in the right hemispheres is in accord with the findings in the literature (23,56), it is not clear what might have determined a shift in

the lateralisation of the effect related to increased semantic control. One possibility is that the neural incongruency effect is not observed in the left hemisphere because neural responses in these regions may have been too transient to be captured by fMRI.

Thus, the involvement of the right parietal and frontal regions may reflect the recruitment of domain-general WM (60,61) and inhibitory control mechanisms (62) applied when incongruences are detected across paragraphs of text. Particularly, the right ventral IFG (BA47) and the right insula might enact the sustained suppression of the incorrect interpretation of the ambiguous word and all the words semantically related to it, after a change of semantic context is detected (63).

The left pMTG modulates semantic activation to focus on aspects of meaning that are appropriate to the task or context (18). Accordingly, we were expecting that this region would also respond to shifts of semantic context. However, this effect was observed in the right pMTG that has different structural and functional connectivity properties as compared to the left pMTG (64,65). For instance, Neurosynth (http://old.neurosynth.org/;66) shows that resting-state co-activation maps from the left and right pMTG regions have different patterns of connectivity with the ATL. That is, the left, but not the right pMTG, shows intrinsic connectivity with the ATL semantic hub. Instead, the right pMTG shows connectivity with regions that, except for the left pMTG, constitute a right lateralised fronto-parietal network. This observation along with evidence that this area is not involved in semantic tasks (18), unless they involve formation of time-extended contextual associations (65), may indicate that the right pMTG plays a critical role in capturing changes of context-sensitive meaning over longer periods of time, possibly by integrating information across WM (frontal and parietal corticies) and semantic networks (left pMTG).

The role of the left AG: semantic hub or buffering system?

Our results reveal that a portion of the left AG (vPGa) supports meaning formation during time-extended semantic cognition similar to the MTG. In fact, an effect of semantic coherence was observed in the anterior ventral portion of the left AG (vPGa). At first sight, this result aligns with the proposal that the left AG has a crucial role for semantic representations (37,67,68). However, this general semantic role for the AG does not fit with a series of findings from neurological patients that have reported semantic impairments after ATL but not parietal damage (see 7) and the demonstrations of equal (de) activation for non-semantic and semantic tasks in this region (19,32,42,46).

Recent compelling evidence has led to an alternative proposal on the role of the left AG that would reconcile neuroimaging and neuropsychological findings. Rather than a hub for semantic integration, the left AG might support a domain-general mechanism that buffers time-, context-, and

space-varying inputs (32,42,46). Since buffering becomes relevant only when the task requires combinations across multiple (internal or external) items (e.g., during encoding, integration, recollection, etc.), it is not surprising that left AG is positively engaged in our study and in other semantic tasks that involve integration of multiple items (40,69).

Beyond the Semantic Network

Besides brain areas implicated in semantic cognition, we also expected to observe additional brain regions and networks reflecting the demands posed by computing and resetting conceptual contexts. In accord with previous findings (3,4,6,20,21,22,23), a set of brain regions comprising the hippocampus, the PCC/precuneus and the DMN AG region (i.e., mid-PGp) responded to semantic integration (LC&HC>NC conditions). Similar to the mid-PGp, these other regions have been identified as nodes of both task-positive (e.g., episodic memory, mind-wandering, etc.) and task-negative (DMN) networks, and have been related to multiple cognitive functions, including semantic cognition (70). Unlike previous studies (3,4,6), activity in the hippocampus, the PCC/precuneus and the mid-PGp (see above) was not modulated by the semantic content per se, but rather by the presence of the contextual support. Given this observation, the neural responses in these areas may reflect encoding and/or retrieval of contextual information (54,71,72).

Finally, contrary to what has been suggested by previous investigations (24,25), DMN regions (e.g., PCC/precuneus and mSFG) were not increasingly engaged by shifts of semantic or task contexts. These inconsistencies might be due to substantial differences in the tasks employed in our and other studies. Being a naturalistic task, the reading task was quite "passive" and resetting the task context did not require the cognitive manipulation (retrieval, inhibition, etc.) of instructions/rules associated to the task to be performed. Instead, switching between the highly novel tasks employed in previous studies (24,25) necessarily involves this sort of process, given that each stimulus domain (i.e., stimuli depicting people, buildings, words) was associated to two possible classification rules (male/female and old/young for face stimuli; skyscraper/cottage and inside/outside view for building stimuli; first letter and last letter for word stimuli). Hence, the task-switch activity observed in DMN regions in previous studies may reflect the retrieval of task rules, rather than reinstatement and assessment of contextual representations. A related possibility is that given the novelty of these tasks (learned prior to scanning), the DMN region activations reflect episodic retrieval of the task instructions.

The Functional Networks

ICA was employed in addition to univariate analysis to reveal how different brain regions were recruited for semantic integration. In the present study, ICA revealed a network sensitive to semantic control demands (SLN), a network sensitive to context integration (ECN) and two networks sensitive to domain-general attentional control demands (HVN and PVN). Finally, ICA revealed also a DMN network modulated by task-condition difficulty.

SLN and ECN: semantic control and working memory processes

In accord to previous research work (e.g., 6,20,21,22,26) and an influential model of semantic cognition (7), we expected two task-positive networks to support semantic processing and executive control. We were expecting these two networks to be modulated by semantic integration (LC& HC>NC) and shifts of semantic context (LC>HC). According to our predictions, ICA revealed a SLN and ECN, both positively engaged during the semantic task conditions.

The SLN network, including semantic, but also MD and other extra-semantic areas, was maximally recruited during shifts of semantic context. This finding suggests that resetting the semantic system requires the orchestration of different neurocomputational mechanisms possibly including WM, semantic processing and domain-general executive control.

The ECN network, including a set of fronto-parietal and medial regions was also positively engaged during the reading task. However, rather than being sensitive to variations of semantic context, the ECN was sensitive to context integration in general. That is, it was positively recruited when the target conditions could be integrated with a previous context, independently of whether the context was highly congruent with the target. Instead, this network was disengaged when information could not be integrated with a previous context. The spatial distribution of this network - including some key nodes identified as WM areas from GLM analysis - and its sensitivity to contextual integration is consistent with a WM function (e.g., 39).

The visual networks support domain-general attentional control mechanisms

ICA analysis revealed that two additional networks were positively engaged during the reading task. These networks, including visual areas, but also other cortical and subcortical control regions (e.g., IFG, pMTG, Precentral gyrus, Putamen, etc.), were strongly engaged during changes of task and semantic context. This result is particularly interesting because it shows that sensory-dorsal and posterior attentional networks are involved in narrative reading and support control functions that are important, but not specific, for semantic integration.

Furthermore, FNC analyses revealed that HVN and PVN were both positively connected to the SLN and negatively connected to the DMN and ECN. We proposed that this coupling might reflect the need of strongly engaging semantic areas after the number reading task, and at the same time, disengaging areas not relevant for the switch of task context, e.g., ECN. Our result revealed that switching efficiently between tasks was related to stronger negative coupling between HVN and DMN and at the same time, enhanced positive coupling between HVN and SLN. According to the DMN-downregulation hypothesis described above, the negative correlations between task-positive HVN and task-negative DMN (34,35) may suggest that the visual network was constantly engaged during the task (except during rest). This is not surprising since HVN and PVN include visual areas and other control structures that are constantly active during the reading tasks and maximally engaged during increased control demands.

The role of DMN

We expected recruitment of a DMN including hippocampus, AG (mid-PGp), PCC/precuneus, and other medial prefrontal structures (73). According to the hypothesis that DMN supports semantic integration (37), we should have observed task-positive responses. However, like previous findings, the DMN showed the typical task-negative response (19,26,27).

A second hypothesis is that the DMN supports episodic retrieval and buffering (38,39,40,41). If so, then one would expect to observe an activation profile similar to the ECN: positively engaged only for conditions allowing integration (LC and HC). Conversely, not only was the DMN negatively engaged during meaning integration (HC and LC), but it also did not show differential responses between conditions preceded (LC) and not preceded by a contextual support (NC). Thus, this result is inconsistent with the proposal that DMN supports episodic retrieval and buffering during narrative reading.

A final and third hypothesis is that the DMN is involved in cognitive transitions by reinstating context-relevant information (24,25). As such one would expect the DMN to be sensitive to a major switch to a new task (NC condition), when a completely different context representation is reawakened. In contrast to this prediction, we found larger task-negative activations for NC as compared with HC.

So what role does the DMN plays in narrative processing, if any? We found that the pattern of DMN activation mirrors that of RTs (Figure 1). This finding suggests that the DMN is sensitive to task-condition difficulty (19,31). Thus it is possible that brain structures not critical for the task may be deactivated to save metabolic energy consumption, in a way proportional to task difficulty (32,74).

4. Materials and Methods

4.1. Participants

Twenty-four volunteers took part in the study (average age=22, SD=2; N female=18). All participants were native English speakers with no history of neurological or psychiatric disorders and normal or corrected-to-normal vision. As a result of technical issues during the scanning session, only data from 22 participants (average age=22, SD=2; N female=18) were usable for fMRI data analyses.

4.2. Stimuli

A total of 40 narrative pairs, each one composed by two paragraphs, were created for the experimental study. For each narrative pair, the same second paragraph (target) was preceded by different first paragraphs (contexts) that could be either high-congruent (i.e., HC) or low-congruent (i.e., LC) with the target in terms of meaning. Both HC and LC context paragraphs could be integrated with the targets, though a reworking of the evolving semantic context was required after LC contexts only, because of a shift in the semantic context (see Table S1 for an example of the stimuli). Homonym words (e.g., bank) were employed in order to determine the exact point in the paragraph in which the shift in the semantic context should have been experienced.

To ensure that HC and LC conditions differed in respect to semantic associative strength between contexts and targets, we quantified in different ways semantic relatedness between the contexts and targets for both HC and LC conditions. First, we employed Latent Semantic Analysis (LSA) (75,76,77), a method measures the semantic relationship between words based on the degree to which they are used in similar linguistic contexts. Hence, for each narrative pair, pairwise LSA values were calculated for contexts and targets and then averaged within both. As result, an LSA value reflecting the associative strength between the context and target was obtained for both conditions. Results from LSA confirmed that semantic associative strength between the (same) target and the context was higher for HC (average score=0.4, SD=0.14) than LC conditions (average score=0.25, SD=0.09) [$t(78)=-5.435$, $p<0.001$].

Second, we asked to a group of independent participants to indicate how much contexts and targets were perceived as being semantically related (0 to 5 scale). The results of this pre-experimental rating suggested that HC (average score=4.4, SD=0.4) and LC (average score=2.3, SD=0.4) conditions were different [$t(9)=-10.626$, $p<0.001$]. Moreover, to ensure that participants could perceive the shift of semantic context during the study, at end of each narrative the question “Was there any change of semantic context between part1 and part2?” was posed. Only pairs of narratives on which at least the 90% of participants responded correctly to the questions were employed in the study.

Finally, another condition was included in the design in order to measure the semantic integration processes in general. Precisely, in the NC condition the target (the same as in HC and LC conditions) was preceded by a string of numbers that could include from one to four-digit numbers.

4.3. Task procedures

There were 40 items per condition presented using an event-related design with the most efficient ordering of events determined using Optseq (http://www.freesurfer.net/optseq). Rest time was intermixed between trials and varied between 2 and 12 seconds (s) (average=3.7, SD=2.8) during which a red fixation cross was presented. The red colour was used in order to mark the end of each trial (each narrative composed by a context and a target). A black fixation cross was presented between contexts and targets and its duration varied between 0 and 6s (average=3, SD=1.6). Each context paragraph was presented for 9s followed by the target for 6s.

Participants were asked to read silently both contexts (verbal material and numbers) and targets (only verbal material). Our volunteers were instructed to press a button when arriving to the end of each paragraph (for both contexts and targets). The instruction emphasized speed, but also the need to understand the meaning of verbal contexts and targets, since at the end of some of the trials participants would have been asked to answer to some questions on the content of the narratives. We specified that in order to perform this task it would have been necessary to integrate the meaning between contexts and targets. Hence, following 13% of the trials a comprehension task was presented to ensure that participants were engaged in the task. When this happened, the target item was followed by a question displayed on the screen for 6s at which participants were required to provide a response (true/false) via button press. A fixation cross between the target and the question was presented during a time that varied between 0 and 6s (average=3.5, SD=2.2). Before starting the experimental study, all participants provided informed consent and were given written instructions. Then they underwent to a practice session with few trials in order to allow them to familiarise with the task. The stimuli used in the practice session were different from those used in the experimental study.

4.4. Task acquisition parameters

Images were acquired using a 3T Philips Achieva scanner using a dual gradient-echo sequence, which is known to have improved signal relative to conventional techniques, especially in areas associated with signal loss (78). Thus, 31 axial slices were collected using a TR=2s, TE=12 and 35 milliseconds (ms), flip angle=95°, 80 x 79 matrix, with resolution 3 x 3mm, slice thickness 4mm. For each participant, 1492 volumes were acquired in total, collected in four runs of 746s each.

4.5. Data analysis

Behavioural data analyses

Behavioural analyses were performed on RTs and the percentage of given responses (omissions). Two separate repeated-measures ANOVAs, one for RTs and the other for percentage of given responses, with "Condition" as within-subjects factor with three levels (NC, LC and HC conditions) were conducted. Bonferroni correction for multiple comparisons was applied to assess statistically significant effects.

fMRI data analyses

Preprocessing

The dual-echo images were averaged. Data was analysed using SPM8. After motion-correction images were co-registered to the participant's T1 image. Spatial normalisation into MNI space was computed using DARTEL (79), and the functional images were resampled to a 3 x 3 x 3mm voxel size and smoothed with an 8mm FWHM Gaussian kernel.

GLM

The data was filtered using a high-pass filter with a cut-off of 128s and then analysed using a GLM. At the individual subject level, each condition was modelled with a separate regressor (Target NC, Target LC and Target HC) with time derivatives added, and events were convolved with the canonical hemodynamic response function. The number reading paragraph condition (Context NC) was also modelled as a regressor of interest in order to have an active baseline against which to compare the semantic tasks. Also the other context paragraphs and comprehension task were modelled as separate regressors of no interest. Each condition was modelled as a single event. Motion parameters were entered into the model as covariates of no interest.

The Semantic Network

To identify the brain areas involved in semantic processing during the narrative reading task, we assessed the whole-brain contrast of semantic target conditions (NC, LC, HC collapsed) against rest and against the number reading task (Context NC condition). All the contrasts were corrected for multiple comparisons with a voxel-wise false discovery rate (FDR) threshold set at $q<0.05$ (80) and a contiguity threshold ≥30 voxels.

Having identified the semantic network, we conducted ROI analyses to assess the functional contribution of key semantic areas in respect to our task manipulations. All the ROI coordinates were

independently derived from the literature (Table S3). Regarding the parietal ROIs, we investigated the functional role of three different portions of the AG (42,46). We employed 10mm spheres for these analyses. Repeated-measures ANOVAs, one for each ROI, with "Condition" as within-subjects factor with three levels (NC, LC and HC targets) were conducted. Bonferroni correction for multiple comparisons was applied to assess statistically significant effects.

Whole-brain univariate analyses of the differences between experimental conditions

Semantic integration effect. To investigate the semantic integration effect the contrasts LC>NC and HC>NC were computed via whole-brain analysis. All the contrasts were corrected for multiple comparisons with a voxel-wise FDR threshold set at $q<0.05$ and a contiguity threshold ≥30 voxels.

Shift of semantic and task contexts. The shift of semantic context effect was established by running whole-brain analysis for the contrast LC>HC. To reveal brain regions that are important for task switches into language from a non-language task (i.e., shift of task context), we also conducted a NC>HC whole-brain contrast. Also these contrasts were corrected for multiple comparisons with a voxel-wise FDR correction threshold set at $q<0.05$ and a contiguity threshold ≥30 voxels.

Importantly, whole-brain contrast analyses alone do not inform on whether the observed differential activation is originated by task-positive or task-negative activation disparities. Hence, the precise contribution of each area was established by conducting ROI analysis (via repeated-measure ANOVAs as above) on a set of key regions revealed by the whole-brain univariate analyses above. In this analysis we opted for 8mm spheres in order to restrict our ROIs only to voxels found to be significantly activated in the univariate contrasts.

Task group spatial ICA

Spatial ICA applied to fMRI data identifies temporally coherent networks by estimating maximally independent spatial sources, referred to as spatial maps (SMs), from their linearly mixed fMRI signals, referred to as TCs. The pre-processed fMRI data was analysed in a group spatial ICA using the GIFT toolbox (http://mialab.mrn.org/software/gift) (81) to decompose the data into its components. GIFT was used to concatenate the subjects' data, and reduce the aggregated data set to the estimated number of dimensions using principal component analysis (PCA), followed by an ICA analysis using the Infomax algorithm (82). Subject-specific SMs and TCs were estimated using GICA back-reconstruction method based on PCA compression and projection (81).

The number of IC estimated within the data was 38. The estimation was achieved by using the Minimum Description Length criteria, first per each individual data-set and then computing the group

mean. The obtained 38 IC were inspected in order to exclude from the analysis artefactual and noise-related components. Similar to previous studies (26,83) the criterion for assigning components as artefact was based on the SMs attained as a result of the one sample t-tests (threshold for voxel-wise significance was set at $p<0.05$, corrected for family-wise error (FWE), and a contiguity threshold ≥ 30 voxels). The SMs were visually compared with the SPM grey matter template. Only components that had the majority of activity within the grey matter were selected (N=22).

Establishing task-related FNs. The 22 ICs were labelled according to the resting state networks template provided in the GIFT toolbox. Then, a multiple regression analysis (implemented as "temporal sorting" function in GIFT) between IC and task model's TCs for each participant was conducted and allowed to identify the ICs related to target conditions (task-related FNs). For that, for each participant the design matrix used for the GLM analysis, where rest periods were modelled implicitly as task baseline, was employed. For each IC, the multiple regression analysis generated 3 beta-weight values (one for each condition NC, LC, and HC) that were averaged across runs and participants. Beta-weight values represent the correlations between TCs of the ICs and the canonical hemodynamic response model for each task condition. These values are thought to reflect engagement of the FNs during specific task conditions (84).

Once extracted the beta weights for each IC associated with each condition, task-relatedness for each IC was assessed by testing group means of averaged beta weights for each task-condition against zero (one-sample t-tests, $p<0.05$). Hence, a positive/negative beta-weight significantly different from zero indicates increase/decrease in activity of the IC during a specific task condition relative to the baseline condition (i.e., rest). Once established the task-related FNs, for each FN a repeated-measures ANOVA was used to assess the main differences between beta weights across different task-conditions. Bonferroni correction for multiple comparisons was applied to assess statistically significant effects.

FNC analysis. To investigate the relationship between task-related FNs, we conducted a FNC analysis using the Mancovan toolbox in GIFT. Hence, FNC was estimated as the Pearson's correlation coefficient between pairs of TCs (85). Subject specific TCs were detrended and despiked based on the median absolute deviation as implemented in 3dDespike (http://afni.nimh.nih.gov/), then filtered using a fifth-order Butterworth low-pass filter with a high frequency cutoff of 0.15 Hz. Pairwise correlations were computed between TCs, resulting in a symmetric $c1 \times c1$ correlation matrix for each subject. For all FNC analyses, correlations were transformed to z-scores using Fisher's transformation, $z=\text{atanh}(k)$, where k is the correlation between two component TCs. One sample t-tests (corrected for multiple comparisons at a $\alpha=0.01$ significance level using FDR) were conducted on task-related FNs in order to reveal the significance of pairwise correlations.

Data Sharing. The data, materials and code will be made available at http://www.mrc-cbu.cam.ac.uk/publications/opendata/.

ACKNOWLEDGEMENTS. This work was supported by a Medical Research Council Programme Grant (MR/R023883/1), an European Research Council Advanced Grant (GAP: 670428 - BRAIN2MIND_NEUROCOMP) and a Postdoctoral Fellowship from the European Union's Horizon 2020 research and innovation programme, under the Marie Sklodowska-Curie grant agreement No 658341.

References

1. Price AR, Bonner MF, Peelle JE, Grossman M (2015) Converging evidence for the neuroanatomic basis of combinatorial semantics in the angular gyrus. J Neurosci 35:3276–3284
2. Price AR, Peelle JE, Bonner MF, Grossman M, Hamilton RH (2016) Causal Evidence for a Mechanism of Semantic Integration in the Angular Gyrus as Revealed by High-Definition Transcranial Direct Current Stimulation. J Neurosci 36:3829–3838.
3. Hasson U, Yang E, Vallines I, Heeger DJ, Rubin N (2008) A hierarchy of temporal receptive windows in human cortex. J Neurosci 28:2539–2550.
4. Lerner Y, Honey CJ, Silbert LJ, Hasson U (2011) Topographic mapping of a hierarchy of temporal receptive windows using a narrated story. J Neurosci 31:2906–2915.
5. Tylén K, et al. (2015) Brains striving for coherence: Long-term cumulative plot formation in the default mode network. Neuroimage, 121:106–114.
6. Simony E, et al. (2016) Dynamic reconfiguration of the default mode network during narrative comprehension. Nat Commun 7:12141.
7. Lambon Ralph MA, Jefferies E, Patterson K, Rogers TT (2017) The neural and computational bases of semantic cognition. Nat Rev Neurosci 18:42.
8. Lambon Ralph MA, Sage K, Jones RW, Mayberry EJ (2010) Coherent concepts are computed in the anterior temporal lobes. Proc Natl Acad Sci USA 107:2717–2722.
9. Rogers TT, et al. (2004) Structure and deterioration of semantic memory: A neuropsychological and computational investigation. Psychol Rev 111:205–235.
10. Hoffman P, McClelland JL, Lambon Ralph MA (2018) Concepts, control, and context: A connectionist account of normal and disordered semantic cognition. Psychological review, 125:293.
11. Chen L, Ralph MAL, Rogers TT (2017) A unified model of human semantic knowledge and its disorders. Nat Hum Behav 1:0039.
12. Brennan J, Pylkkänen L (2012) The time-course and spatial distribution of brain activity associated with sentence processing. Neuroimage 60:1139–1148.
13. Pallier C, Devauchelle A-D, Dehaene S (2011) Cortical representation of the constituent structure of sentences. Proc Natl Acad Sci USA 108:2522–2527.
14. Humphries C, Binder JR, Medler DA, Liebenthal E (2006) Syntactic and semantic modulation of neural activity during auditory sentence comprehension. J Cogn Neurosci 18:665–679.

15. Noppeney U, Price CJ (2004) An FMRI study of syntactic adaptation. J Cogn Neurosci 16:702–713.
16. Vandenberghe R, Nobre AC, Price CJ (2002) J Cogn Neurosci 14:550–560.
17. Jefferies E, Lambon Ralph MA (2006) Semantic impairment in stroke aphasia versus semantic dementia: a case-series comparison. Brain 129:2132–2147.
18. Noonan KA, Jefferies E, Visser M, Lambon Ralph MA (2013) Going beyond inferior prefrontal involvement in semantic control: Evidence for the additional contribution of dorsal angular gyrus and posterior middle temporal cortex. J Cogn Neurosci 25:1824–1850.
19. Humphreys GF, Hoffman P, Visser M, Binney RJ, Lambon Ralph MA (2015) Establishing task-and modality-dependent dissociations between the semantic and default mode networks. Proc Natl Acad Sci USA 112:7857–7862.
20. Silbert LJ, Honey CJ, Simony E, Poeppel D, Hasson U (2014) Coupled neural systems underlie the production and comprehension of naturalistic narrative speech. Proc Natl Acad Sci USA 111:E4687–E4696.
21. Price CJ (2012) A review and synthesis of the first 20years of PET and fMRI studies of heard speech, spoken language and reading. Neuroimage 62:816–847.
22. Vigneau M, et al. (2006) Meta-analyzing left hemisphere language areas: Phonology, semantics, and sentence processing. Neuroimage 30:1414–1432.
23. Xu J, Kemeny S, Park G, Frattali C, Braun A (2005) Language in context: Emergent features of word, sentence, and narrative comprehension. Neuroimage 25:1002–1015.
24. Crittenden BM, Mitchell DJ, Duncan J (2015) Recruitment of the default mode network during a demanding act of executive control. eLife 4:e06481.
25. Smith V, Mitchell DJ, Duncan J (2018) Role of the default mode network in cognitive transitions. Cereb Cortex 28:3685–3696.
26. Geranmayeh F, Wise RJS, Mehta A, Leech R (2014) Overlapping networks engaged during spoken language production and its cognitive control. J Neurosci 34:8728–8740
27. Wirth M, et al. (2011) Semantic memory involvement in the default mode network: A functional neuroimaging study using independent component analysis. Neuroimage 54:3057–3066.
28. Beckmann CF, DeLuca M, Devlin JT, Smith SM (2005) Investigations into resting-state connectivity using independent component analysis. Philos Trans R Soc London B 360:1001–1013.
29. Seeley, et al. (2007) Dissociable intrinsic connectivity networks for salience processing and executive control. J Neurosci 27:2349–2356.

30. Hoffman P, Binney RJ, Lambon Ralph MA (2015) Differing contributions of inferior prefrontal and anterior temporal cortex to concrete and abstract conceptual knowledge. Cortex 63:250–266.
31. Vatansever D, Menon DK, Stamatakis EA (2017) Default mode contributions to automated information processing. Proc Natl Acad Sci USA 114:12821–12826.
32. Humphreys GF, Lambon Ralph MA (2017) Mapping domain-selective and counterpointed domain-general higher cognitive functions in the lateral parietal cortex: evidence from fMRI comparisons of difficulty-varying semantic versus visuo-spatial tasks, and functional connectivity analyses. Cereb Cortex 27:4199–4212.
33. Spreng RN, Stevens WD, Chamberlain JP, Gilmore AW, Schacter DL (2010) Default network activity, coupled with the frontoparietal control network, supports goal directed cognition. Neuroimage 53:303–317.
34. Vincent JL, Kahn I, Snyder AZ, Raichle ME, Buckner RL (2008) Evidence for a frontoparietal control system revealed by intrinsic functional connectivity. J Neurophysiol 100:3328–3342.
35. Fox MD, et al. (2005) The human brain is intrinsically organized into dynamic, anticorrelated functional networks. Proc Natl Acad Sci USA 102:9673–9678.
36. Dixon ML, et al. (2017) Interactions between the default network and dorsal attention network vary across default subsystems, time, and cognitive states. Neuroimage 147:632–649.
37. Binder JR, Desai RH, Graves WW, Conant LL (2009) Where is the semantic system? A critical review and meta-analysis of 120 functional neuroimaging studies. Cereb Cortex 19:2767–2796
38. Vilberg KL, Rugg MD (2008) Memory retrieval and the parietal cortex: a review of evidence from a dual-process perspective. Neuropsychologia 46:1787–1799.
39. Vatansever D, Manktelow AE, Sahakian BJ, Menon DK, Stamatakis EA (2017) Angular default mode network connectivity across working memory load. Hum Brain Mapp 38:41–52.
40. Van der Linden M, Berkers RM, Morris RG, Fernández G (2017) Angular gyrus involvement at encoding and retrieval is associated with durable but less specific memories. J Neurosci 3603–16.
41. Rugg MD, Vilberg KL (2013) Brain networks underlying episodic memory retrieval. Curr Opin Neurobiol 23:255–260.
42. Humphreys GF, Lambon Ralph MA (2015) Fusion and fission of cognitive functions in the human parietal cortex. Cereb Cortex 25: 3547–3560.
43. Rice GE, Lambon Ralph MA, Hoffman P (2015) The roles of left versus right anterior temporal lobes in conceptual knowledge: An ALE meta-analysis of 97 functional neuroimaging studies. Cereb Cortex 25:4374–4391.

44. Visser M, Lambon Ralph MA (2011) Differential contributions of bilateral ventral anterior temporal lobe and left anterior superior temporal gyrus to semantic processes. J Cogn Neurosci 23:3121–3131.
45. Seghier ML, Fagan E, Price CJ (2010) Functional subdivisions in the left angular gyrus where the semantic system meets and diverges from the default network. J Neurosci 30:16809–16817.
46. Humphreys GF, Jackson RL, Lambon Ralph MA (2019) Overarching principles and dimensions of the functional organisation in the inferior parietal cortex. bioRxiv: 654178. Preprint, Posted May 31, 2019.
47. Duncan J (2010) The multiple-demand (MD) system of the primate brain: Mental programs for intelligent behaviour. Trends Cogn Sci 14:172–179.
48. Kucyi A, Esterman M, Riley CS, Valera EM (2016) Spontaneous default network activity reflects behavioral variability independent of mind-wandering. Proc Natl Acad Sci USA 113:13899–13904.
49. Esterman M, Noonan SK, Rosenberg M, Degutis J (2013) In the zone or zoning out? Tracking behavioral and neural fluctuations during sustained attention. Cereb Cortex 23:2712–2723.
50. Patterson K, Nestor PJ, Rogers TT (2007) Where do you know what you know? The representation of semantic knowledge in the human brain. Nat Rev Neurosci 8:976–987.
51. Binney RJ, Parker GJM, Lambon Ralph MA (2012) Convergent connectivity and graded specialization in the rostral human temporal lobe as revealed by diffusion-weighted imaging probabilistic tractography. J Cogn Neurosci 24:1998–2014.
52. Dundon NM, et al. (2017) Human Parahippocampal Cortex Supports Spatial Binding in Visual Working Memory. Cereb Cortex 28:3589–3599.
53. Bar M, Aminoff E, Schacter DL (2008) Scenes unseen: The parahippocampal cortex intrinsically subserves contextual associations, not scenes or places per se. J Neurosci 28:8539–8544.
54. Davachi L (2006) Item, context and relational episodic encoding in humans. Curr Opin Neurobio 16:693–700.
55. Griffiths BJ, et al. (2018) Hippocampal synchrony and neocortical desynchrony cooperate to encode and retrieve episodic memories. bioRxiv: 305698. Preprint, Posted August 01, 2018.
56. Jung-Beeman M (2005) Bilateral brain processes for comprehending natural language. Trends Cogn Sci 9:512–518.
57. Hickok G, Poeppel D (2007) The cortical organization of speech processing. Nat Rev Neurosci 8:393– 402.

58. Poeppel D (2003) The analysis of speech in different temporal integration windows: cerebral lateralization as 'asymmetric sampling in time'. Speech Commun 41:245–255.
59. St George M, Kutas M, Martinez A, Sereno MI (1999) Semantic integration in reading: engagement of the right hemisphere during discourse processing. Brain 122:1317–1325.
60. Gajardo-Vidal A, et al. (2018) How right hemisphere damage after stroke can impair speech comprehension. Brain 141:3389–3404.
61. Vigneau, et al. (2011) What is right-hemisphere contribution to phonological, lexico-semantic, and sentence processing?: Insights from a meta-analysis. Neuroimage 54:577–593.
62. Aron AR, Robbins TW, Poldrack RA (2004) Inhibition and the right inferior frontal cortex. Trends Cogn Sci 8:170–177.
63. Mason RA, Just MA (2007) Lexical ambiguity in sentence comprehension. Brain Res 1146:115–127.
64. Vassal F, et al. (2016) Combined DTI tractography and functional MRI study of the language connectome in healthy volunteers: extensive mapping of white matter fascicles and cortical activations. PLoS One 11:e0152614.
65. Xu J, et al. (2015) Tractography-based parcellation of the human middle temporal gyrus. Sci Rep 5:18883.
66. Yarkoni T, Poldrack RA, Nichols TE, Van Essen DC, Wager, TD (2011) Large-scale automated synthesis of human functional neuroimaging data. Nat methods 8:665.
67. Geschwind N (1972) Language and Brain. Sci Am 226:76-&.
68. Binder JR, Desai RH (2011) The neurobiology of semantic memory. Trends Cogn Sci 15:527–536.
69. Price CJ, Mechelli A (2005) Reading and reading disturbance. Curr Opin Neurobiol 15:231–8.
70. Krieger-Redwood K, et al. (2016) Down but not out in posterior cingulate cortex: Deactivation yet functional coupling with prefrontal cortex during demanding semantic cognition. Neuroimage 141:366–377.
71. Spaniol J, et al. (2009) Event-related fMRI studies of episodic encoding and retrieval: Meta-analyses using activation likelihood estimation. Neuropsychologia 47:1765–1779.
72. Staudigl T, Hanslmayr S (2013) Theta oscillations at encoding mediate the context-dependent nature of human episodic memory. Curr Biol 23:1101–1106.
73. Andrews-Hanna JR, Reidler JS, Sepulcre J, Poulin R, Buckner RL (2010) Functional-anatomic fractionation of the brain's default network. Neuron 65:550–562.

74. Attwell D, Laughlin SB (2001) An energy budget for signaling in the grey matter of the brain. J Cereb Blood Flow Metab 21:1133–1145.
75. Hoffman P (2019) Reductions in prefrontal activation predict off-topic utterances during speech production. Nat Commun 10:515.
76. Hoffman P, Lambon Ralph MA, Rogers TT (2013) Semantic diversity: a measure of semantic ambiguity based on variability in the contextual usage of words. Behav Res Methods 45:718–730.
77. Landauer TK, Dumais ST (1997) A solution to Plato's problem: The latent semantic analysis theory of acquisition, induction, and representation of knowledge. Psychol Rev 104:211.
78. Halai AD, Welbourne SR, Embleton K, Parkes LM (2014) A comparison of dual gradient-echo and spin-echo fMRI of the inferior temporal lobe. Hum Brain Mapp 35:4118–4128.
79. Ashburner J (2007) A fast diffeomorphic image registration algorithm. Neuroimage 38:95–113.
80. Benjamini Y, Hochberg Y (1995) Controlling the False Discovery Rate: A Practical and Powerful Approach to Multiple Testing. J R Statist Soc B 57:289–300.
81. Calhoun VD, Adali T, Pearlson GD, Pekar JJ (2001) A method for making group inferences from functional MRI data using independent component analysis. Hum Brain Mapp 14:140–151.
82. Bell AJ, Sejnowski TJ (1995) An information-maximization approach to blind separation and blind deconvolution. Neural Comput **7**:1129–1159.
83. Griffanti, et al. (2017) Hand classification of fMRI ICA noise components. Neuroimage 154:188–205.
84. Xu J, et al. (2013) Task-related concurrent but opposite modulations of overlapping functional networks as revealed by spatial ICA. Neuroimage 79:62–71.
85. Jafri MJ, Pearlson GD, Stevens M, Calhoun VD (2008) A method for functional network connectivity among spatially independent resting-state components in schizophrenia. Neuroimage 39:1666-1681.

Figure 1. Behavioural results for **(A)** reading times and **(B)** percentage of given responses for NC, LC and HC target conditions. Error bars correspond to Standard Error (SE).

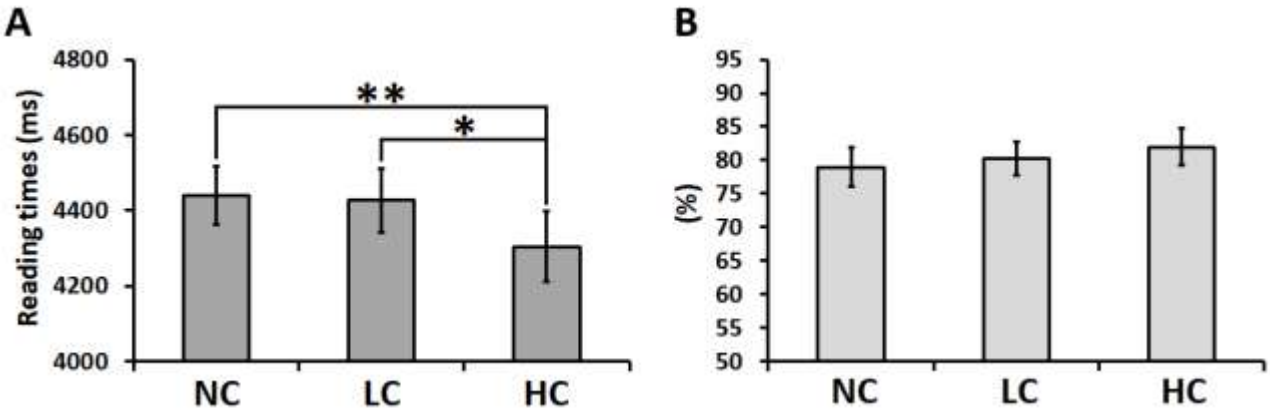

Figure 2. GLM results for target conditions against passive and active baselines and for different ROIs (derived from the literature) including **(A)** the ATL **(B)** the left AG and **(C)** the semantic control network. Mean beta values for each task condition were compared against rest. Error bars correspond to SE.

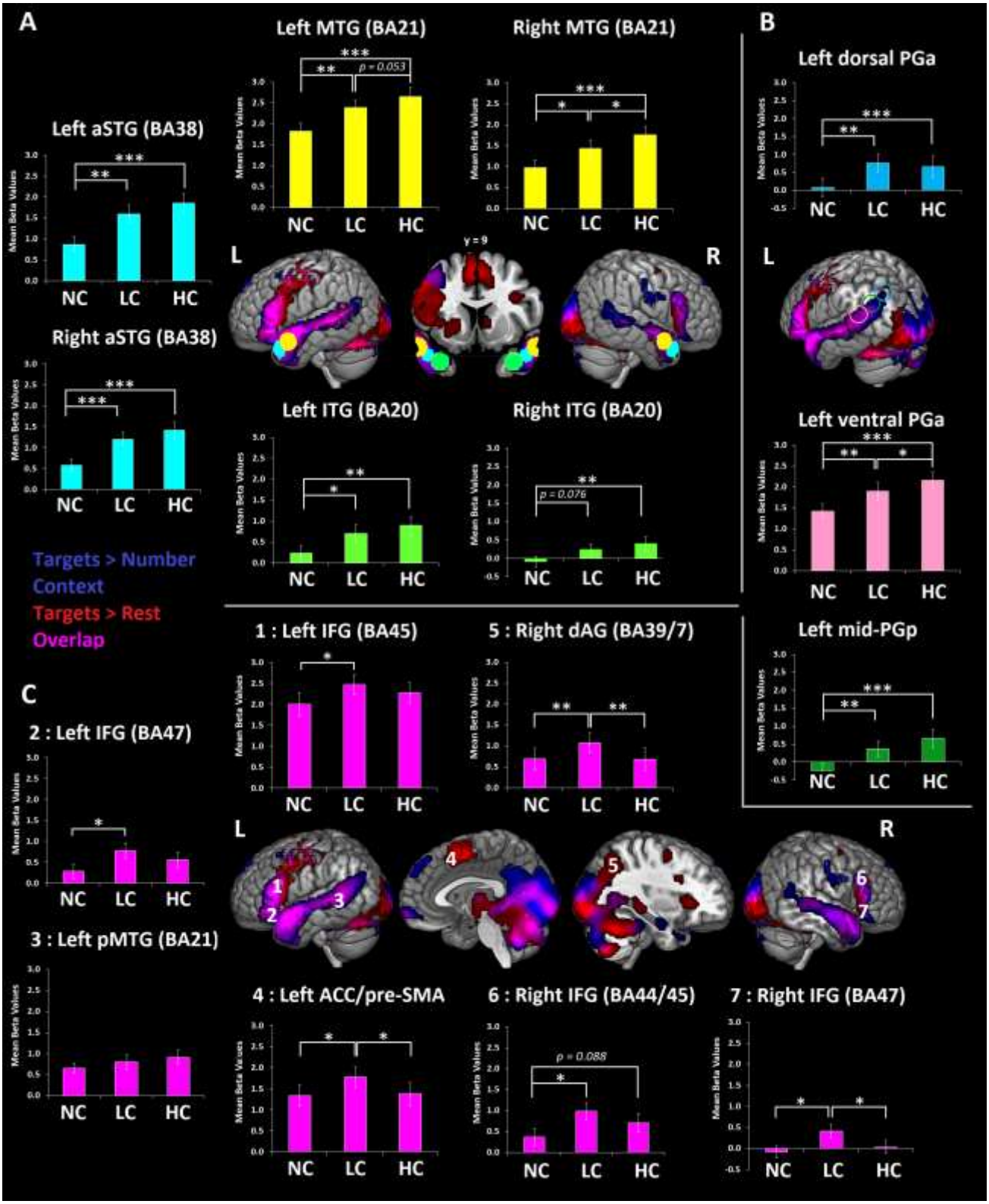

Figure 3. GLM results for **(A)** the semantic integration effect (HC&LC>NC) and five ROIs (derived from the peaks of activation in areas of overlap). GLM results for **(B)** the shift of semantic and task context effects (LC>HC and NC>HC, respectively) and six ROIs derived from the peaks of activation. Error bars correspond to SE.

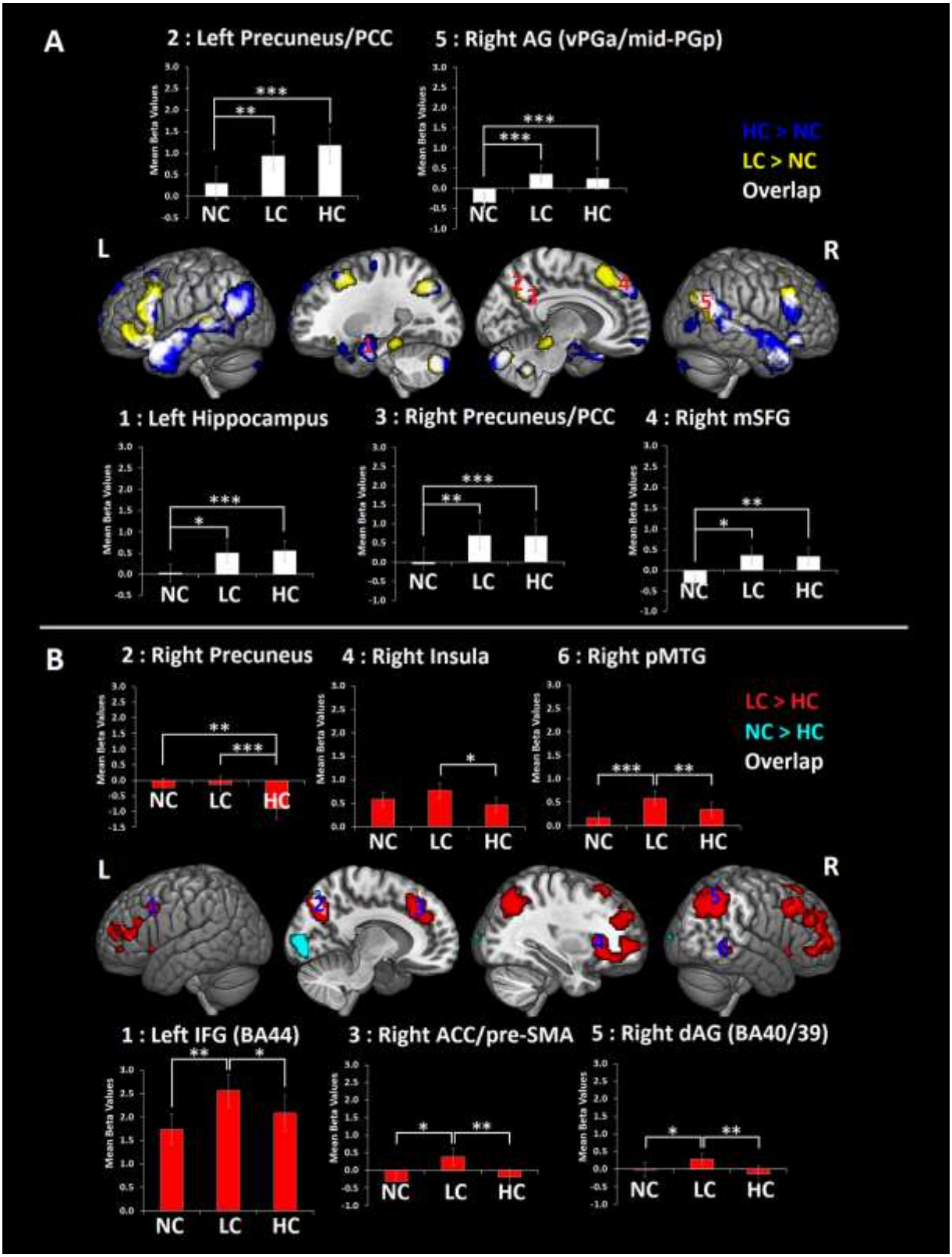

Figure 4. Task-related FNs and beta-weights' results. **(A)** Semantic language network (SLN); **(B)** Executive control network (ECN); **(C)** Higher visual network (HVN); **(D)** Primary visual network (PVN); **(E)** Default-mode network (DMN). Error bars correspond to SE.

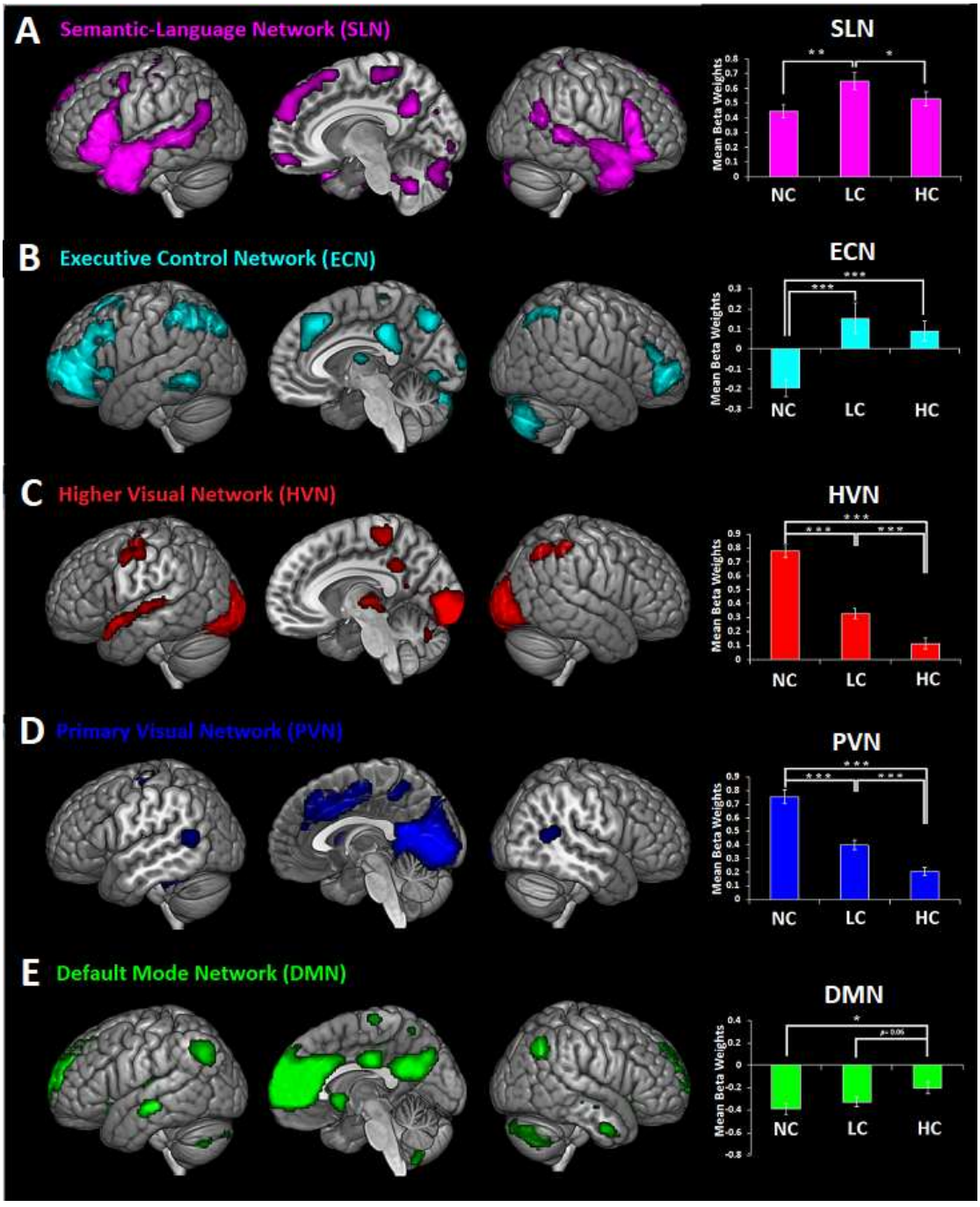

Supplementary Information for

Revealing the neural networks that extract conceptual gestalts from continuously evolving or changing semantic contexts

Francesca M. BRANZI, Gina F. HUMPHREYS, Paul HOFFMAN, and Matthew A. LAMBON RALPH

Francesca M. Branzi or Matthew A. Lambon Ralph
Email: Francesca.Branzi@mrc-cbu.cam.ac.uk or Matt.Lambon-Ralph@mrc-cbu.cam.ac.uk

This PDF file includes:

Figure S1.

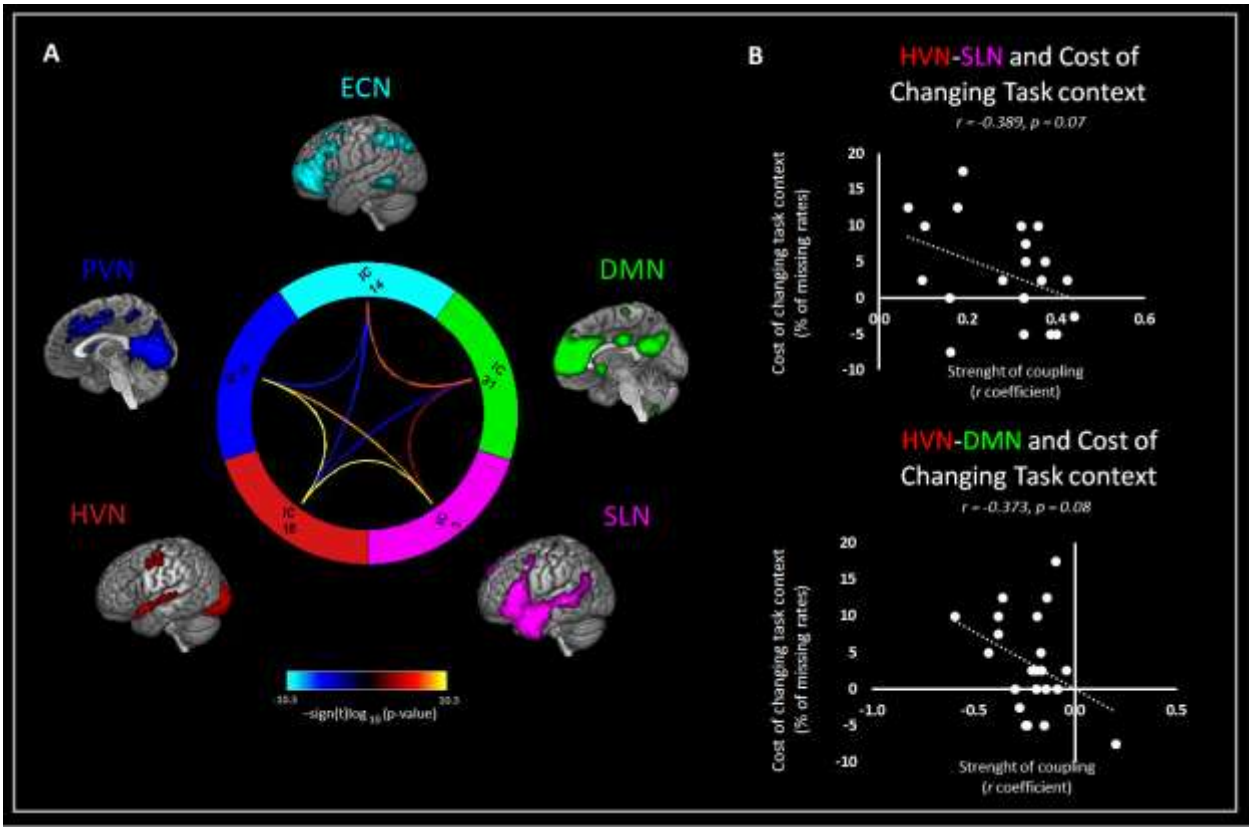

FNC results. (A) Connectogram of the FNC results: Significant pairwise correlations ($p<0.05$) were corrected for multiple comparisons (FDR, $\alpha = 0.01$). Significance and direction of each pairwise correlation is displayed as the $-\text{sign}(t)\log10(p)$; and **(B)** Correlations between strength of coupling and the behavioural cost associated with changes of task context.

Table S1. Examples of stimuli for High−Congruent and Low−Congruent conditions (Context and Target paragraphs). The shift of semantic context after Low−congruent contexts was expected to be perceived after the critical ambiguous word, here depicted in red.

(1) High−congruent context: *We learnt many things that day. We learnt about elephants and the natural disaster in Tanzania. Indeed, two major climatic changes had drastically affected the number of elephants.*
(1) Low−congruent context: *We discovered many things that week. We were told about the rainforest and the environmental disaster in Peru. Indeed, three major oil spills had drastically affected the trees of the rainforest.*
(1) Target: We also learnt that trunks can be used by elephants to rub an itchy eye. Moreover, these animals use their trunk to threaten and to throw objects, and as snorkels when swimming in water
(2) High−congruent context: *This famous psychologist was explaining the causes of wrongful convictions throughout history. It seemed that it was a social minority problem. He had to work hard to prove this. Joe was watching the TV very carefully.*
(2) Low−congruent context: *This famous driver was explaining that his car had a problem which made it slow. It seemed that it was a fuel system problem. The team had to work hard to fix it. Jamie was watching the TV very carefully.*
(2) Target: The expert said that race is one aspect of social biases that leads to discriminatory behaviours. This psychologist was saying that these biases can affect people's lives dramatically.
(3) High−congruent context: *The garden is a nice place to stay in summer and she spends some time there. She takes care of the flowers and she covers her skin. Unfortunately, she knows very well that it is necessary.*
(3) Low−congruent context: *The garden is a great place to stay in spring and she spends many hours there. She takes care of the plants and she places traps near the small holes in the ground. Unfortunately, she knows very well that it is necessary.*
(3) Target: Given the large number of moles on her skin she has to be careful with the sun. The doctor told her that she should wear a large hat on her head while she is doing these activities.

Table S2. MNI coordinates and locations of the activation peaks from the GLM analyses. GLM results were FDR−corrected voxel−wise at a statistical threshold of $q<0.05$, and a contiguity threshold ≥30 voxels.

Contrast	cluster size	T	x	y	z	Location
Semantic Targets > Number Context (against rest)	17923	23.86	12	−87	−3	R Lingual Gyrus
		23.49	-6	-93	-6	L Calcarine Gyrus
		19.52	18	-93	6	R Superior Occipital Gyrus
	167	7.61	-3	66	-12	L Mid Orbital Gyrus
		3.77	-6	48	-18	L Rectal Gyrus
	472	5.61	-9	54	42	L Superior Frontal Gyrus
		5.26	-6	18	63	L Posterior-Medial Frontal
		5.15	-6	57	33	L Superior Medial Gyrus
	310	4.34	-45	-21	21	L Rolandic Operculum
		3.72	-39	-6	18	L Rolandic Operculum
	30	3.27	-3	-9	51	L Posterior-Medial Frontal
Semantic Targets > rest	20217	19.12	−18	−90	−9	L Occipital cortex (Area hOc3v [V3v])
		16.9	18	−93	−6	R Calcarine Gyrus
		16.27	−6	−93	−6	L Calcarine Gyrus
	61	6.41	−3	66	−15	L Mid Orbital Gyrus
	115	4.28	33	0	54	R Middle Frontal Gyrus
		3.38	45	3	57	R Middle Frontal Gyrus
	52	4.11	-9	51	36	L Superior Medial Gyrus
High-Congruent > No-Context (against rest)	1302	8.93	48	9	−30	R Medial Temporal Pole
		8.13	51	6	−21	R Medial Temporal Pole
		8.12	66	−6	−18	R Middle Temporal Gyrus
	397	8.33	−9	−51	36	L Precuneus
		6.58	9	−57	36	R Precuneus
	2354	8.25	−48	−66	27	L Angular Gyrus (PGp)
		7.93	−54	−60	24	L Angular Gyrus (PGa)
		7.26	−39	−66	36	L Angular Gyrus (PGp)
	394	7.83	21	−81	−42	R Cerebelum
	142	6.27	60	21	27	R IFG p. Opercularis
	193	5.64	−21	−9	−21	L Hippocampus

		4.57	−36	−12	−30	L Fusiform Gyrus
	228	5.22	−21	−78	−39	L Cerebelum
	82	5.03	6	−57	−45	R Cerebelum
		4.05	−6	−60	−45	L Cerebelum
	345	4.92	3	48	39	L Superior Medial Gyrus
		4.05	15	54	42	R Superior Medial Gyrus
		3.91	−9	21	57	L Posterior-Medial Frontal
	46	4.71	−9	69	6	L Superior Medial Gyrus
	217	4.64	−33	21	51	L Middle Frontal Gyrus
		4.13	−36	6	48	L Precentral Gyrus
	45	4.51	0	60	−15	L Rectal Gyrus
		3.41	18	63	−12	R Superior Orbital Gyrus
	155	4.43	−54	21	12	L IFG p. Triangularis
		4.13	−54	21	27	L IFG p. Triangularis
	38	4.08	24	−9	−21	R Hippocampus
	31	4	51	−78	3	R Middle Occipital Gyrus
		3.46	54	−72	9	R Middle Temporal Gyrus
	49	3.88	33	−33	−18	R Fusiform Gyrus
		3.61	39	−27	−18	R Fusiform Gyrus
	162	3.88	−27	−15	63	L Precentral Gyrus
		3.59	−57	−18	36	L Postcentral Gyrus
		3.36	−54	−18	48	L Postcentral Gyrus
	76	3.76	−39	−24	18	L Rolandic Operculum
Low-Congruent > No-Context (against rest)	292	7.02	15	−78	−33	R Cerebelum
	863	6.92	39	−60	30	R Angular Gyrus (PGa)
		4.93	54	−60	27	R Angular Gyrus (PGp)
		4.52	54	−36	3	R Middle Temporal Gyrus
	322	6.21	3	24	57	L Posterior-Medial Frontal
		3.8	6	45	42	R Superior Medial Gyrus
	252	5.91	48	12	−30	R Medial Temporal Pole
		5.06	57	6	−30	R Middle Temporal Gyrus
		4.25	48	27	−15	R IFG p. Orbitalis
	154	5.32	57	21	33	R IFG p. Opercularis
	203	5.27	−39	−24	18	L Rolandic Operculum
		5.07	−33	−33	18	L Rolandic Operculum
		2.91	−54	−18	6	L Superior Temporal Gyrus
	336	5.24	−6	−57	−42	L Cerebelum
		4.96	−12	−75	−30	L Cerebelum
		4.92	9	−54	−45	R Cerebelum
	810	5.03	−27	−69	42	L Inferior Parietal Lobule
		4.99	−60	−60	21	L Angular Gyrus (PGp)
		4.77	−33	−69	33	L Middle Occipital Gyrus

	1402	4.85	−45	21	−24	L Temporal Pole
		4.7	−27	12	48	L Middle Frontal Gyrus
		4.65	−60	−6	−9	L Middle Temporal Gyrus
	300	4.56	12	−54	33	R Precuneus
		4.25	−3	−60	45	L Precuneus
		4.2	6	−60	42	R Precuneus
	110	4.17	−12	−33	−15	L Cerebelum
		3.81	−24	−36	−18	L Fusiform Gyrus
		3.18	−12	−45	−24	L Cerebelum
	66	4.01	−39	−12	−27	L Inferior Temporal Gyrus
		3.5	−30	−9	−27	L ParaHippocampal Gyrus
	70	3.97	9	−30	−15	R Cerebelum
		3.39	18	−36	−15	R Cerebelum
		2.69	27	−33	−18	R Fusiform Gyrus
	49	3.19	33	12	45	R Middle Frontal Gyrus
	30	3.16	33	57	12	R Superior Frontal Gyrus
	67	3.15	−39	−21	39	L Postcentral Gyrus
		2.77	−54	−18	36	L Postcentral Gyrus
Low-Congruent > High-Congruent (against rest)	430	6.49	3	30	42	L Superior Medial Gyrus/ACC-preSMA
		5.54	9	27	36	R Middle Cingulate Cortex
		5.19	3	24	54	L Posterior-Medial Frontal
	1123	6.36	12	−72	42	R Precuneus
		5.87	48	−54	33	R Angular Gyrus (PGa)
		5.25	42	−51	45	R Inferior Parietal Lobule (IPS)
	76	5.22	−30	33	−12	L IFG p. Orbitalis
		3.55	−39	48	−6	L Middle Orbital Gyrus
	995	5.14	39	51	−3	R Middle Orbital Gyrus
		4.95	30	27	−9	R IFG p. Orbitalis
		4.86	30	24	6	R Insula Lobe
	53	4.79	60	−42	−6	R Middle Temporal Gyrus
	194	4.77	−45	12	33	L Precentral Gyrus
		4.35	−42	3	27	L Precentral Gyrus
	164	4.73	−51	39	9	L IFG p. Triangularis
		4.53	−54	30	24	L IFG p. Triangularis
		4.1	−36	57	18	L Middle Frontal Gyrus
	77	3.92	−36	15	−3	L Insula Lobe
		3.88	−39	15	9	L Insula Lobe
	39	3.69	24	27	60	R Superior Frontal Gyrus
		3.5	30	21	57	R Middle Frontal Gyrus
No-Context > High-Congruent	148	6.53	24	−96	6	R Middle Occipital Gyrus

(against rest)						
		5.99	15	−87	−6	R Lingual Gyrus
	50	6.05	15	−66	36	R Precuneus
		4.35	9	−72	54	R Precuneus/Superior Parietal Lobe
	55	5.63	0	−30	24	Posterior Cingulate Cortex

L=left; R=right; IFG=inferior frontal gyrus

Table S3. MNI coordinates for ROIs derived from the literature.

ROI groups	Study	Type of Analysis	x	y	z	Location
Temporal lobe	Rice et al., 2015 (see 1)	Activation likelihood clusters from the GingerALE analyses (Verbal input modality studies)	±48	16	−28	aSTG (BA38)
			±58	8	−20	MTG (BA21)
			±36	12	−34	ITG (BA20)
Semantic control network	Noonan et al., 2013 (see 2)	Activation likelihood clusters from the GingerALE analyses (High > Low Semantic Control Studies)	−45	19	21	L IFG (BA45/44)
			−35	22	−11	L IFG (BA47)
			−55	−50	−5	L pMTG (BA21/37/20)
			−3	16	49	L ACC/pre−SMA (BA32/ 24/8/6)
			36	−63	39	R dAG (BA39/7)
			35	22	−11	R IFG (BA47)
			47	22	29	R IFG (BA44/45)
Left AG	Humphreys et al., 2019 (see 3)	Task ICA	−48	−69	36	L mid−PGp
			−33	−72	46	L dPGa
			−51	−54	21	L vPGa

L=left; R=right; a=anterior, p=posterior; d=dorsal; v=ventral; STG=superior temporal gyrus; MTG=middle temporal gyrus; ITG=inferior temporal gyrus; IFG=inferior frontal gyrus; ACC/pre−SMA=anterior cingulate cortex/pre−supplementary motor area; AG=angular gyrus.

Table S4. MNI coordinates and locations of the activation peaks for each task−related FN. The results were FWE−corrected voxel−wise at a statistical threshold of $p<0.05$, and a contiguity threshold ≥30 voxels.

Component	cluster size	T	x	y	z	Location
SLN	5601	34.49	−51	−9	−12	L Superior Temporal Gyrus
		32.23	−57	−6	−21	L Middle Temporal Gyrus
		28.71	−51	24	12	L IFG (p. Triangularis)
	443	22.11	6	−57	30	R Precuneus
		16.28	−6	−57	33	L Precuneus
		9.95	−18	−48	36	L Precuneus
	1142	22.09	−3	54	27	L Superior Medial Gyrus
		21.86	−9	51	36	L Superior Medial Gyrus
		19.83	−6	15	63	L Posterior−Medial Frontal
	2657	21.09	48	33	−15	R IFG (p. Orbitalis)
		20.42	45	15	−24	R Temporal Pole
		19.61	57	24	−3	R IFG (p. Orbitalis)
	232	20.28	6	−57	−42	R Cerebelum (IX)
		18.43	−6	−57	−45	L Cerebelum (IX)
		9.53	12	−42	−33	R Cerebelum
	579	19.76	21	−75	−30	R Cerebelum (Crus 1)
		17.98	21	−81	−39	R Cerebelum (Crus 2)
		14.17	18	−81	−21	R Cerebelum (Crus 1)
	1017	15.66	−12	−27	66	L Paracentral Lobule
		14.16	−33	−21	66	L Precentral Gyrus
		13.33	−33	−36	63	L Postcentral Gyrus
	155	13.17	6	57	−15	R Rectal Gyrus
	194	12.81	−18	−75	−30	L Cerebelum (Crus 1)
		12.48	−18	−81	−39	L Cerebelum (Crus 2)
	60	11.82	15	−84	9	R Calcarine Gyrus
		9.75	12	−72	12	R Calcarine Gyrus
	71	11.25	33	−93	15	R Middle Occipital Gyrus
		10.57	27	−84	24	R Superior Occipital Gyrus
	53	10.13	15	−54	−3	R Lingual Gyrus
	63	9.46	−12	−51	−6	L Lingual Gyrus
	48	8.37	−39	−48	−18	L Inferior Temporal Gyrus
ECN	4313	30.45	−45	48	−3	L Middle Orbital Gyrus
		25.96	−33	54	0	L Middle Frontal Gyrus
		25.42	−45	48	−12	L Middle Orbital Gyrus
	1229	28.17	−51	−45	48	L Inferior Parietal Lobule (IPS)
		24.67	−33	−72	45	L Inferior Parietal Lobule (dPGa)
		23.08	−36	−57	39	L Angular Gyrus (IPS)

	341	22.14	−6	−30	36	L Middle Cingulate Cortex
		10.75	−15	−51	18	L Precuneus
	1054	20.96	30	−66	−36	R Cerebelum (Crus 1)
		19.99	12	−81	−27	R Cerebelum (Crus 1)
		19,97	27	−81	−51	R Cerebelum (Crus 2)
	263	16.53	−60	−51	−6	L Middle Temporal Gyrus
		10.03	−63	−33	−15	L Middle Temporal Gyrus
	136	16.38	−6	−72	42	L Precuneus
	184	13.84	42	−60	54	R Angular Gyrus (IPS/PGa)
		11.78	51	−48	54	R Inferior Parietal Lobule (PFm)
	106	13.09	−15	−27	60	L Primary Motor Cortex
	593	12.58	48	51	0	R Middle Frontal Gyrus
		12.25	45	48	−12	R IFG (p. Orbitalis)
		11.85	39	42	−9	R Middle Orbital Gyrus
	82	11.83	−9	−42	0	L Lingual Gyrus
	193	10.38	−9	−102	12	L Superior Occipital Gyrus
		9.91	−15	−72	−3	L Lingual Gyrus
		9.59	−6	−75	−6	L Lingual Gyrus
	34	9.50	−27	−36	−21	L Fusiform Gyrus
	54	9.00	63	−51	−6	R Middle Temporal Gyrus
		8.93	63	−45	−15	R Inferior Temporal Gyrus
	56	8.43	21	−99	15	R Superior Occipital Gyrus
HVN	3420	34.08	15	−90	−3	R Lingual Gyrus
		32.40	−9	−90	−3	L Calcarine Gyrus
		25.54	−12	−93	−18	L Lingual Gyrus
	785	14.26	−18	−30	0	L Thalamus
		13.26	−60	−30	6	L Middle Temporal Gyrus
		12.49	−30	−6	3	L Putamen
	197	12.61	12	−36	57	R Paracentral Lobule
		10.49	−6	−33	57	L Paracentral Lobule
		8.63	−9	−27	66	L Paracentral Lobule
	38	12.03	24	−30	0	R Thalamus (Temporal)
	204	10.86	−51	0	42	L Precentral Gyrus
		9.54	−54	−15	48	L Postcentral Gyrus
		8.61	−33	−18	51	L Precentral Gyrus
	155	10.85	51	−60	51	R Angular Gyrus (PGa)
		8.37	57	−42	57	R Inferior Parietal Lobule (PFm)
		7.27	48	−45	42	R Supra Marginal Gyrus
	101	10.84	3	−30	39	R Middle Cingulate Cortex
		9.91	−3	−42	33	L Posterior Cingulate Cortex
	59	8.64	18	−57	42	R Precuneus
	66	8.16	−9	66	9	L Superior Medial Gyrus
		7.60	9	66	3	R Superior Medial Gyrus
		7.50	0	63	0	L Superior Medial Gyrus

PVN	5332	34.97	0	−87	0	L Calcarine Gyrus
		32.36	−6	−72	6	L Calcarine Gyrus
		31.92	−18	−57	12	L Calcarine Gyrus
		7.42	39	33	−24	R IFG (p. Orbitalis)
	775	14.48	0	15	36	L Middle Cingulate Cortex
		13.69	0	0	45	L Middle Cingulate Cortex
		13.20	9	24	36	R Middle Cingulate Cortex
	120	13.74	9	6	6	R Caudate Nucleus
		8.51	12	−15	12	R Thalamus
	154	12.21	−3	−42	51	L Middle Cingulate Cortex
		7.49	−3	−63	54	L Precuneus
	157	10.93	−39	−24	51	L Postcentral Gyrus
		10.56	−36	−24	69	L Precentral Gyrus
	36	10.77	−6	6	6	L Caudate Nucleus
	40	10.74	−54	−3	−18	L Middle Temporal Gyrus
	108	10.30	−42	18	30	L IFG (p. Triangularis)
		7.62	−36	6	36	L Middle Frontal Gyrus
	32	9.81	60	18	−9	R Temporal Pole
		8.55	54	15	−15	R Temporal Pole
	44	9.53	42	3	42	R Precentral Gyrus
		8.41	36	12	48	R Middle Frontal Gyrus
		6.79	42	15	36	R IFG (p. Opercularis)
		8.82	−33	39	−21	L IFG (p. Orbitalis)
	34	8.51	−24	24	39	L Middle Frontal Gyrus
DMN	4772	42.13	−6	36	9	L Anterior Cingulate Cortex
		39.02	−9	60	15	L Superior Medial Gyrus
		35.16	6	45	3	R Anterior Cingulate Cortex
	737	21.28	3	−51	27	R Posterior Cingulate Cortex
		19.76	3	−18	30	R Middle Cingulate Cortex
		16.73	−6	−63	24	L Cuneus
	101	16.96	−66	−21	−12	L Middle Temporal Gyrus
	85	15.44	−33	15	−18	L IFG (p.Orbitalis) / Insula Lobe
	197	15.12	−48	−63	36	L Angular Gyrus (PGa/PGp)
	111	13.02	54	−60	39	R Inferior Parietal Lobule
	324	12.99	30	−81	−30	R Cerebelum (Crus 1)
		11.96	39	−75	−39	R Cerebelum (Crus 2)
		11.31	45	−54	42	R Inferior Parietal Lobule
	90	12.17	45	−63	−42	R Cerebelum (Crus 2)
		8.81	−33	−81	−33	L Cerebelum (Crus 2)
	71	11.97	30	18	−15	R Insula Lobe
	245	11.81	−24	−24	−15	L Subiculum
		10.99	−51	−12	0	L Superior Temporal Gyrus
		9.80	−54	−27	12	L Superior Temporal Gyrus
	54	11.65	51	−3	−33	R Inferior Temporal Gyrus
	51	11.19	6	−60	−57	R Cerebelum (IX)

	119	10.01	−15	−30	66	L Paracentral Lobule
		9.00	−6	−21	69	L Paracentral Lobule
		8.00	33	−18	69	R Precentral Gyrus

L=left; R=right; IFG=inferior frontal gyrus; SLN=semantic language network; ECN=executive control network; HVN=higher visual network; PVN=primary visual network; DMN=default-mode network.

References

1. Rice GE, Lambon Ralph MA, Hoffman P (2015) The roles of left versus right anterior temporal lobes in conceptual knowledge: An ALE meta-analysis of 97 functional neuroimaging studies. Cereb Cortex 25:4374–4391.
2. Noonan KA, Jefferies E, Visser M, Lambon Ralph MA (2013) Going beyond inferior prefrontal involvement in semantic control: Evidence for the additional contribution of dorsal angular gyrus and posterior middle temporal cortex. J Cogn Neurosci 25:1824–1850.
3. Humphreys GF, Jackson RL, Lambon Ralph MA (2019) Overarching principles and dimensions of the functional organisation in the inferior parietal cortex. bioRxiv: 654178. Preprint, Posted May 31, 2019.